arXiv:1410.4390v1 [physics.optics] 16 Oct 2014

Coherent supercontinuum generation in a silicon photonic wire in the telecommunication wavelength range

François Leo,[1,2,*] **Simon-Pierre Gorza,**[3] **Stéphane Coen,**[4] **Bart Kuyken,**[1,2] **and Gunther Roelkens**[1,2]

[1] *Photonics Research Group, Department of Information Technology, Ghent University-IMEC, Ghent B-9000, Belgium*
[2] *Center for Nano- and Biophotonics (NB-photonics), Ghent University, Belgium*
[3] *OPERA-Photonique, Université Libre de Bruxelles (ULB), 50 Av. F. D. Roosevelt, CP 194/5, B-1050 Bruxelles, Belgium*
[4] *Physics Department, The University of Auckland, Private Bag 92019, Auckland 1142, New Zealand*
[*] *Corresponding author: francois.leo@intec.ugent.be*

Compiled October 17, 2014

We demonstrate a fully coherent supercontinuum spectrum spanning 500 nm from a silicon-on-insulator photonic wire waveguide pumped at 1575 nm wavelength. An excellent agreement with numerical simulations is reported. The simulations also show that a high level of two-photon absorption can essentially enforce the coherence of the spectral broadening process irrespective of the pump pulse duration. © 2014 Optical Society of America

OCIS codes: (130.4310) Integrated optics, Nonlinear; (190.5530) Nonlinear optics, Pulse propagation and temporal solitons

Supercontinuum generation is a well known phenomenon that leads to the generation of broadband light through the nonlinear spectral broadening of narrowband sources [1]. It has been studied and demonstrated in a plethora of materials and platforms, and is now a key process for the design of broadband light sources for many applications, such as high-precision frequency metrology [2], optical coherence tomography [3], telecommunication [4], or short pulse synthesis [5].

For many applications, however, bandwidth is not everything, and the coherence of the generated light is also important [6–8]. In photonic crystal fibers (PCFs), which have proved very popular for supercontinuum generation, a general criterium to obtain coherent spectra has been developed. The coherence is highly dependent on the fiber dispersion, and on the duration and peak power of the input pulse which can be seen as a high-order soliton [9]. A simple distinction can be made between the "long" pulse regime (with input soliton order $N > 16$) where noise-induced modulation instability (MI) dominates, leading to incoherent supercontinua, and the "short" pulse regime (with $N < 10$) where the process is driven by initial pulse compression followed by soliton fission [10], and in which the coherence of the pump is preserved [11].

Supercontinuum generation has also recently been investigated experimentally in several chip-scale integrated nonlinear optical platforms [12–17]. In some of these experiments using short pump pulses, soliton fission was experimentally demonstrated [14, 17]. In particular, soliton dynamics has been observed in silicon-on-insulator (SOI) waveguides at telecom wavelengths, suggesting that the same mechanisms as that responsible for supercontinuum generation in PCFs can explain broadband emission in silicon waveguides despite the inherently strong two-photon absorption (TPA) [17]. Although the occurrence of soliton fission would suggest good coherence properties, only limited studies of the coherence of supercontinua from integrated devices have been performed so far, based on beat note measurements [18, 19]. A complete characterization of the coherence of such a supercontinuum is however still lacking. In this Letter, we address this point, and we demonstrate the generation of a supercontinuum with high optical coherence across its whole spectrum in an SOI integrated waveguide pumped at telecom wavelengths.

Our experiment is based on a 4 mm-long SOI waveguide with a standard height of 220 nm, a width of 700 nm, and a zero dispersion wavelength located at 1425 nm. It is pumped with an optical parametric oscillator (OPO; Spectra Physics OPAL) generating 150 fs pulses (full width at half maximum, FWHM) at 1575 nm wavelength with a repetition rate ν_{rep} of 82 MHz. Chip incoupling is performed with a microscope objective while the output light is collected by a lensed fiber, as shown at the top of our experimental setup in Fig. 1. With a coupled peak power of 37 W, we observe [Fig. 2(a)] a broadband supercontinuum spectrum covering more than 500 nm of bandwidth. As reported in [17], the spectral broadening is mainly driven by soliton fission and the subsequent emission of dispersive waves. The latter are emitted around 1200 nm wavelength, in the normal dispersion regime [20,21], but their

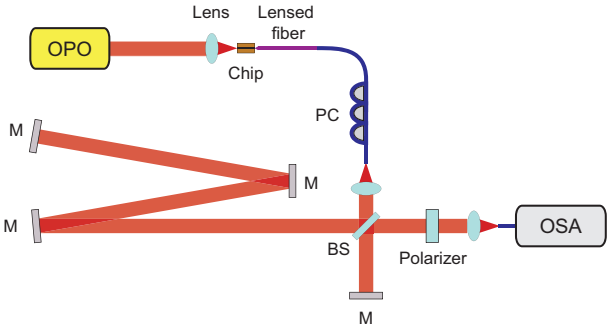

Figure 1. Experimental setup: the SOI waveguide on a chip is pumped by an OPO. The output light is collected by a lensed fiber and sent to an asymmetric Michelson interferometer. The resulting interferogram is recorded on an optical spectrum analyzer (OSA). BS: beam splitter, PC: polarization controller, M: mirror.

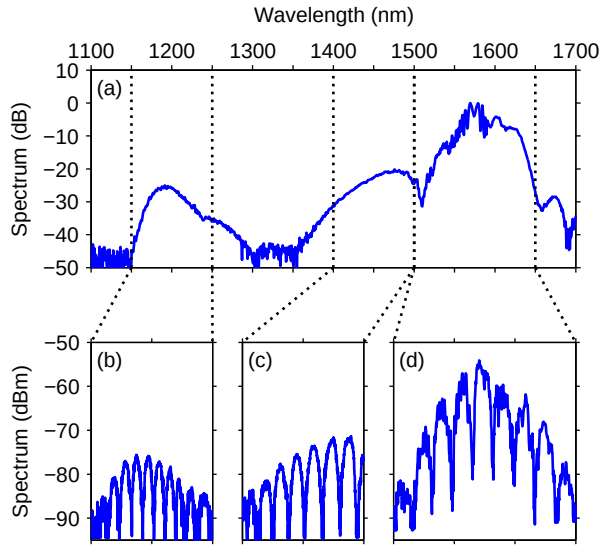

Figure 2. (a) Experimental spectrum (1 nm spectral resolution) at the output of our SOI waveguide, normalized to a peak level of 0 dBm. (b)–(d) Spectral fringes measured at the output of the asymmetric Michelson interferometer with couplings optimized to maximize transmission in, respectively, the 1150–1250 nm, 1400–1500 nm, and 1500–1650 nm spectral windows. The deeply contrasted fringes indicate strong phase coherence.

precise spectral position highly depends on the dispersion profile of the waveguide [17].

In order to study the coherence properties of our supercontinuum spectrum, we resort to the approach pioneered by Bellini and Hänsch [8], and which is based on the observation of spectral interferometric fringes between two independently generated supercontinua. This method has been heavily used for PCF-based supercontinuum generation, first numerically [9] and then experimentally [22–25]. It provides information about the coherence across the whole generated spectrum at once. In our experiment, we use a single SOI waveguide as the supercontinuum source, and the two independently generated supercontinua come from subsequent pump pulses as initially proposed for PCFs in [23]. Accordingly, the light collected at the output of our waveguide is sent to an asymmetric Michelson interferometer (see Fig. 1) with a delay $\tau = 1/\nu_{\mathrm{rep}} + \delta t$ close to the time period between two subsequent pump pulses. The extra delay δt is chosen to have a reasonable density of spectral fringes, but not so high as to be limited by the resolution of the optical spectrum analyzer (OSA). The visibility of the spectral fringes recorded on the OSA was maximized by introducing a polarizer at the output of the interferometer.

Our coherence measurements have been taken separately over three spectral windows (1150–1250 nm, 1400–1500 nm, and 1500–1650 nm) because light is delivered and collected into and out of our bulk interferometer through optical fibers, and the coupling efficiencies depend on wavelength. Figs. 2(b)–(d) show spectral interferograms in these three spectral windows, in each case measured after re-optimizing the couplings. The vertical axis in Figs. 2(b)–(d) directly reflects the actual power density at the output of the interferometer, showing how the OSA noise floor (at -95 dBm) limits our measurements. Spectral fringes spaced by about 10–15 nm are clearly visible in all three windows. The fringe contrast is excellent throughout the spectrum, typically exceeding 20 dB, indicating excellent phase coherence with the pump across the span of our supercontinuum. In particular, we note that the dispersive-wave peak around 1200 nm wavelength is coherent too, despite being effectively separated from the rest of the spectrum.

The coherence of the generated light can be quantified by extracting the fringe visibility as a function of wavelength from our measurements, $V = (I_{\max} - I_{\min})/(I_{\max} + I_{\min})$, where $I_{\max}$ and $I_{\min}$ correspond to the maxima and minima of each of the fringes. The results of these calculations are plotted as red dots in Fig. 3(a), where the corresponding wavelength has been set for each point halfway between the maximum and the minimum of the fringe. Note that the high density of points in that figure results from taking measurements from four independently recorded interferograms in each spectral window. For comparison, Fig. 3(a) also shows the overall generated supercontinuum spectrum [same as in Fig. 2(a)]. We can see that the coherence is very high across the whole spectrum, with an average visibility of 97 % which appears to be limited only by the noise floor of the OSA. Our analysis therefore proves that broad coherent supercontinua can be generated in a silicon photonic wire pumped at telecom wavelengths. We must note that the input soliton order is relatively large in our experiment, $N \simeq 20$. Supercontinua generatd in PCF's are typically incoherent for such large values of N [11]. Here, we believe that coherence can be obtained for larger N because of the large TPA of silicon, which effectively limits the number of solitons that can exist after fission as described in [17].

To understand our results better, we have compared our experimental measurements with stochastic numerical simulations. Our model is based on a nonlinear Schrödinger equation with a complex nonlinear parameter accounting for TPA [$\gamma = (234 + 44i)\ \mathrm{W^{-1}m^{-1}}$], and also includes free carrier absorption (FCA) and free carrier dispersion (FCD). That model was shown in [17] as appropriate for supercontinuum generation in silicon with short pump pulses. Note that apart from the parameters explicitly listed here, we have used the same parameter values as in that earlier work. The degree of first-order coherence $g_{12}^{(1)}$ of the generated light can be evaluated from the classical formula [9, 22]

$$g_{12}^{(1)}(\lambda) = \frac{\langle E_1^*(\lambda) E_2(\lambda)\rangle}{\sqrt{\langle |E_1(\lambda)|^2\rangle \langle |E_2(\lambda)|^2\rangle}}, \qquad (1)$$

where the angle brackets denote ensemble averages over supercontinuum spectra $E_{1,2}(\lambda)$ obtained from separate simulations with different realizations of input noise. In practice, input noise is taken into consideration by adding one photon per mode with random phase to the initial condition. We have performed 20 independent simulations, and the averages were calculated over each pair of calculated output fields. The vis-

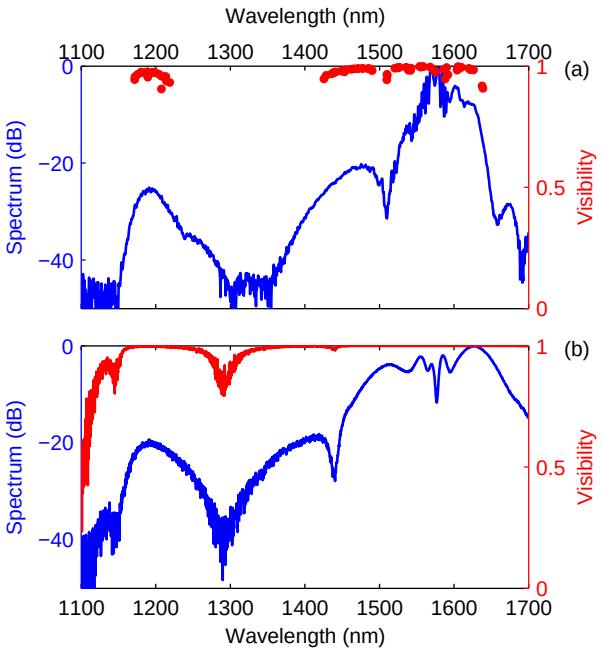

Figure 3. Comparison of (a) experimental and (b) numerical results. Blue: Spectrum at the output of the waveguide. Red: Visibility of spectral fringes, in (a) as observed at the output of our asymmetric Michelson interferometer, and in (b) obtained with stochastic numerical simulations.

ibility of spectral fringes can then be obtained as

$$V(\lambda) = \frac{2\sqrt{I_1(\lambda)I_2(\lambda)}}{I_1(\lambda)+I_2(\lambda)}\left|g_{12}^{(1)}(\lambda)\right| \qquad (2)$$

where $I_{1,2}$ correspond to the averaged spectral intensities of each arm of the interferometer. Note that the fringe visibility constitutes a lower bound of the modulus of the coherence function, and that they are equal only if the powers retrieved from both arms of the interferometer are balanced, which was nearly the case in our experiment.

Our numerical simulation results are presented in Fig. 3(b), in which we show both the average spectral intensity at the waveguide output (blue) and the visibility of spectral fringes (red). Both curves are in excellent agreement with the experimental results [Fig. 3(a)], confirming that spectral broadening in our conditions is independent from input noise. We believe this is the first clear demonstration of supercontinuum coherence in the presence of carrier dynamics. Carriers are well known to highly affect the nonlinear dynamics of silicon wires pumped at telecommunication wavelengths in the case of longer pulses, through both FCD and FCA [26]. As the effect of carriers is much weaker in the femtosecond regime [27], our results allow to envision the use of silicon waveguides to extend frequency combs generated for example by Erbium doped fiber lasers.

To understand further the influence of the nonlinear losses and the pump pulse duration on the coherence of supercontinuum generation in silicon, we have performed additional numerical simulations whose results are summarized in Fig. 4. Here we used 20 W peak power pump pulses and a 1 cm-long waveguide, slightly longer than in our experiment, but otherwise with the same width, thickness, and dispersion parameters as before. The pump pulse duration (FWHM) increases from 150 fs (top, as in our experiment) to 250 fs (middle), and 500 fs (bottom). In the left column, we have used the same nonlinear parameter γ as in Fig. 3, and that corresponds to our experimental conditions. In contrast, results in the right column have been obtained for a reduced TPA, $\gamma = (234+15i)$ W^{-1}m^{-1}, corresponding to a better figure of merit like that found at longer pump wavelengths or in other materials like amorphous silicon [15, 28].

The results shown in the top-left of Fig. 4, with 150 fs pump pulses and high TPA, are similar to our current experiment, i.e., a broad supercontinuum with perfect coherence across the whole bandwidth. We note that the coherence is maintained here despite the longer waveguide considered (1 cm versus 4 mm) and it indicates that the supercontinuum spectrum observed in [17] was also likely fully coherent. As the pump pulse duration increases (left of Fig. 4, middle and bottom graphs), the spectral width of the supercontinuum shrinks, but an excellent coherence is nevertheless maintained across the generated bandwidth. This is in stark contrast with supercontinuum generation in PCF where the coherence is observed to collapse for long pulse durations [11]. As the TPA is reduced (right column), the super-

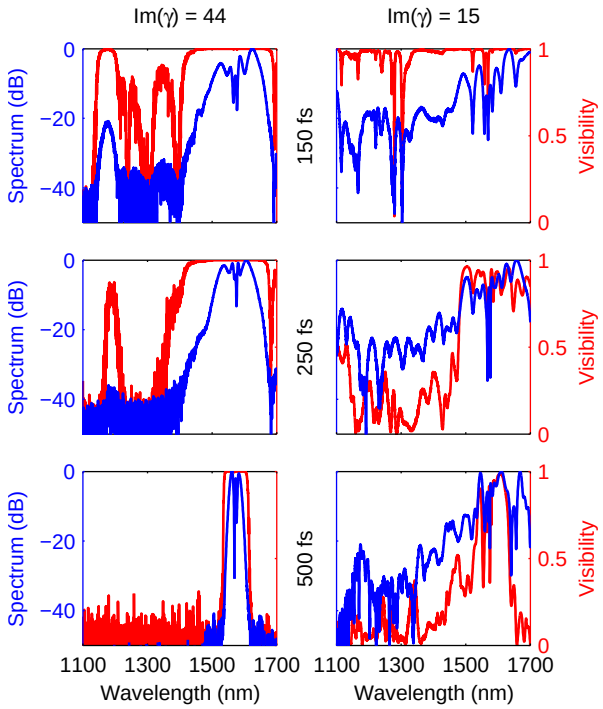

Figure 4. Simulated supercontinuum spectra (blue) and their coherence (visibility, red) for increasing pump pulse durations (from top to bottom, $T_0 = 150$ fs, 250 fs, and 500 fs) and for two different TPA strengths [Im$(\gamma) = 44$ and 15 W^{-1}m^{-1} in the left and right column, respectively]. Waveguide length: 1 cm; Pump peak power: 20 W.

continuum appears broader for all pump pulse duration considered, which is a simple consequence of the lower losses enabling higher power throughout the waveguide. However, in this case, the coherence does severely degrade for the longer pump pulses, with almost no coherence preserved with 500 fs pump pulses.

Overall, TPA seems to enforce the coherence of the supercontinuum generation process. If a spectrum broad enough for one's application can be obtained despite the strong nonlinear losses, it will be coherent, irrespective of pump pulse duration or input soliton order. Our experiment [Fig. 3(a)] hits that sweet spot. However, the spectral broadening quickly saturates with the peak power, and using longer pump pulses lead to a collapse of the spectral width. We can relate these observations to the increase of the fission length for longer pump pulse durations. As the fission is delayed, other mechanisms take over the spectral broadening. In PCF, or waveguides with weak TPA, Modulation instability (MI) kicks in but, being noise driven, leads to poor coherence. High TPA quenches MI, leaving only self-phase modulation, which is a coherent process, but then spectral broadening is limited by the fast nonlinear drop of peak power.

In conclusion, we have studied experimentally and numerically the coherence properties of supercontinuum generation in a silicon wire waveguide pumped at telecommunication wavelengths where the two-photon based nonlinear losses are significant. We have demonstrated a fully coherent 500 nm-wide supercontinuum spectrum, spanning from 1200 nm to 1700 nm. Numerical simulations agree very well with experimental observations and explain the role of TPA. Coherence appears to be preserved because the supercontinuum mainly arises through soliton fission despite the high value of the input soliton order, which is in practice reduced by TPA. Our results also reveal that in our experimental conditions, with relatively short 150 fs pump pulses, free carriers do not significantly affect the spectral broadening nor the coherence of the process.

This work is supported by the Belgian Science Policy Office (BELSPO) Interuniversity Attraction Pole (IAP) programme under grant no. IAP-6/10 and by the FP7-ERC-MIRACLE project. The participation of S. Coen to this project was made possible thanks to a Research & Study Leave granted by The University of Auckland and to a visiting fellowship from the FNRS (Belgium). Bart Kuyken acknowledges the special research fund of Ghent University (BOF) for a fellowship. The authors would like to thank Laurent Olislager for fruitful discussions.

References

1. R. R. Alfano and S. L. Shapiro, Phys. Rev. Lett. **24**, 584 (1970).
2. D. J. Jones, S. A. Diddams, J. K. Ranka, A. Stentz, R. S. Windeler, J. L. Hall, and S. T. Cundiff, Science **288**, 635 (2000).
3. I. Hartl, X. D. Li, C. Chudoba, R. K. Ghanta, T. H. Ko, J. G. Fujimoto, J. K. Ranka, and R. S. Windeler, Opt. Lett. **26**, 608 (2001).
4. S. V. Smirnov, J. D. Ania-Castanon, T. J. Ellingham, S. M. Kobtsev, S. Kukarin, and S. K. Turitsyn, Opt. Fib. Tech. **12**, 122 (2006).
5. A. M. Heidt, J. Rothhardt, A. Hartung, H. Bartelt, E. G. Rohwer, J. Limpert, and A. Tünnermann, Opt. Express **19**, 13873 (2011).
6. M. Nakazawa, K. Tamura, H. Kubota, and E. Yoshida, Opt. Fib. Tech. **4**, 215 (1998).
7. R. Holzwarth, M. Zimmermann, T. Udem, T. W. Hänsch, P. Russbüldt, K. Gäbel, R. Poprawe, J. C. Knight, W. Wadsworth, and P. St. J. Russell, Opt. Lett. **26**, 1376 (2001).
8. M. Bellini and T. W. Hänsch, Opt. Lett. **25**, 1049 (2000).
9. J. M. Dudley and S. Coen, Opt. Lett. **27**, 1180 (2002).
10. A. V. Husakou and J. Herrmann, Phys. Rev. Lett. **87**, 203901 (2001).
11. J. M. Dudley, G. Genty, and S. Coen, Rev. Mod. Phys. **78**, 1135 (2006).
12. I.-W. Hsieh, X. Chen, X. Liu, J. I. Dadap, N. C. Panoiu, C.-Y. Chou, F. Xia, W. M. Green, Y. A. Vlasov, and R. M. Osgood, Opt. Express **15**, 15242 (2007).
13. M. R. Lamont, B. Luther-Davies, D.-Y. Choi, S. Madden, and B. J. Eggleton, Opt. Express **16**, 14938 (2008).
14. R. Halir, Y. Okawachi, J. S. Levy, M. A. Foster, M. Lipson, and A. L. Gaeta, Opt. Lett. **37**, 1685 (2012).
15. J. Safioui, F. Leo, B. Kuyken, S.-P. Gorza, S. K. Selvaraja, R. Baets, Ph. Emplit, G. Roelkens, and S. Massar, Opt. Express **22**, 3089 (2014).
16. D. Y. Oh, D. Sell, H. Lee, K. Y. Yang, S. A. Diddams, and K. J. Vahala, Opt. Lett. **39**, 1046 (2014).
17. F. Leo, S.-P. Gorza, J. Safioui, P. Kockaert, S. Coen, U. Dave, B. Kuyken, and G. Roelkens, Opt. Lett. **39**, 3623 (2014).
18. C. R. Phillips, C. Langrock, J. S. Pelc, M. M. Fejer, J. Jiang, M. E. Fermann, and I. Hartl, Opt. Lett. **36**, 3912 (2011).
19. B. Kuyken, T. Ideguchi, S. Holzner, M. Yan, T. W. Hänsch, J. Van Campenhout, P. Verheyen, S. Coen, F. Leo, R. Baets, G. Roelkens, and N. Picque, arXiv e-print 1405.4205 (2014).
20. N. Akhmediev and M. Karlsson, Phys. Rev. A **51**, 2602 (1995).
21. M. Erkintalo, Y. Q. Xu, S. G. Murdoch, J. M. Dudley, and G. Genty, Phys. Rev. Lett. **109**, 223904 (2012).
22. X. Gu, M. Kimmel, A. P. Shreenath, R. Trebino, J. M. Dudley, S. Coen, and R. S. Windeler, Opt. Express **11**, 2697 (2003).
23. F. Lu and W. Knox, Opt. Express **12**, 347 (2004).
24. D. Türke, S. Pricking, A. Husakou, J. Teipel, J. Herrmann, and H. Giessen, Opt. Express **15**, 2732 (2007).
25. J. W. Nicholson, A. D. Yablon, M. F. Yan, P. Wisk, R. Bise, D. J. Trevor, J. Alonzo, T. Stockert, J. Fleming, E. Monberg, F. Dimarcello, and J. Fini, Opt. Lett. **33**, 2038 (2008).
26. L. Yin and G. P. Agrawal, Opt. Lett. **32**, 2031 (2007).
27. L. Yin, Q. Lin, and G. P. Agrawal, Opt. Lett. **32**, 391 (2007).
28. X. Liu, B. Kuyken, G. Roelkens, R. Baets, R. M. O. Jr, and W. M. J. Green, Nature Photonics **6**, 667 (2012).

References with titles

1. R. R. Alfano and S. L. Shapiro, "Emission in the region 4000 to 7000 Å via four-photon coupling in glass," Phys. Rev. Lett. **24,** 584–587 (1970).
2. D. J. Jones, S. A. Diddams, J. K. Ranka, A. Stentz, R. S. Windeler, J. L. Hall, and S. T. Cundiff, "Carrier-envelope phase control of femtosecond mode-locked lasers and direct optical frequency synthesis," Science **288,** 635–639 (2000).
3. I. Hartl, X. D. Li, C. Chudoba, R. K. Ghanta, T. H. Ko, J. G. Fujimoto, J. K. Ranka, and R. S. Windeler, "Ultrahigh-resolution optical coherence tomography using continuum generation in an air-silica microstructure optical fiber," Opt. Lett. **26,** 608–610 (2001).
4. S. V. Smirnov, J. D. Ania-Castanon, T. J. Ellingham, S. M. Kobtsev, S. Kukarin, and S. K. Turitsyn, "Optical spectral broadening and supercontinuum generation in telecom applications," Opt. Fib. Tech. **12,** 122–147 (2006).
5. A. M. Heidt, J. Rothhardt, A. Hartung, H. Bartelt, E. G. Rohwer, J. Limpert, and A. Tünnermann, "High quality sub-two cycle pulses from compression of supercontinuum generated in all-normal dispersion photonic crystal fiber," Opt. Express **19,** 13873–13879 (2011).
6. M. Nakazawa, K. Tamura, H. Kubota, and E. Yoshida, "Coherence degradation in the process of supercontinuum generation in an optical fiber," Opt. Fib. Tech. **4,** 215–223 (1998).
7. R. Holzwarth, M. Zimmermann, T. Udem, T. W. Hänsch, P. Russbüldt, K. Gäbel, R. Poprawe, J. C. Knight, W. Wadsworth, and P. St. J. Russell, "White-light frequency comb generation with a diode-pumped Cr:LiSAF laser," Opt. Lett. **26,** 1376–1378 (2001).
8. M. Bellini and T. W. Hänsch, "Phase-locked white-light continuum pulses: toward a universal optical frequency-comb synthesizer," Opt. Lett. **25,** 1049–1051 (2000).
9. J. M. Dudley and S. Coen, "Coherence properties of supercontinuum spectra generated in photonic crystal and tapered optical fibers," Opt. Lett. **27,** 1180–1182 (2002).
10. A. V. Husakou and J. Herrmann, "Supercontinuum generation of higher-order solitons by fission in photonic crystal fibers," Phys. Rev. Lett. **87,** 203901/1–4 (2001).
11. J. M. Dudley, G. Genty, and S. Coen, "Supercontinuum generation in photonic crystal fiber," Rev. Mod. Phys. **78,** 1135–1184 (2006).
12. I.-W. Hsieh, X. Chen, X. Liu, J. I. Dadap, N. C. Panoiu, C.-Y. Chou, F. Xia, W. M. Green, Y. A. Vlasov, and R. M. Osgood, "Supercontinuum generation in silicon photonic wires," Opt. Express **15,** 15242–15249 (2007).
13. M. R. Lamont, B. Luther-Davies, D.-Y. Choi, S. Madden, and B. J. Eggleton, "Supercontinuum generation in dispersion engineered highly nonlinear (γ = 10 /W/m) As_2S_3 chalcogenide planar waveguide," Opt. Express **16,** 14938–14944 (2008).
14. R. Halir, Y. Okawachi, J. S. Levy, M. A. Foster, M. Lipson, and A. L. Gaeta, "Ultrabroadband supercontinuum generation in a CMOS-compatible platform," Opt. Lett. **37,** 1685–1687 (2012).
15. J. Safioui, F. Leo, B. Kuyken, S.-P. Gorza, S. K. Selvaraja, R. Baets, Ph. Emplit, G. Roelkens, and S. Massar, "Supercontinuum generation in hydrogenated amorphous silicon waveguides at telecommunication wavelengths," Opt. Express **22,** 3089–3097 (2014).
16. D. Y. Oh, D. Sell, H. Lee, K. Y. Yang, S. A. Diddams, and K. J. Vahala, "Supercontinuum generation in an on-chip silica waveguide," Opt. Lett. **39,** 1046–1048 (2014).
17. F. Leo, S.-P. Gorza, J. Safioui, P. Kockaert, S. Coen, U. Dave, B. Kuyken, and G. Roelkens, "Dispersive wave emission and supercontinuum generation in a silicon wire waveguide pumped around the 1550 nm telecommunication wavelength," Opt. Lett. **39,** 3623–3626 (2014).
18. C. R. Phillips, C. Langrock, J. S. Pelc, M. M. Fejer, J. Jiang, M. E. Fermann, and I. Hartl, "Supercontinuum generation in quasi-phase-matched $LiNbO_3$ waveguide pumped by a Tm-doped fiber laser system," Opt. Lett. **36,** 3912–3914 (2011).
19. B. Kuyken, T. Ideguchi, S. Holzner, M. Yan, T. W. Hänsch, J. Van Campenhout, P. Verheyen, S. Coen, F. Leo, R. Baets, G. Roelkens, and N. Picque, "An octave spanning mid-infrared frequency comb generated in a silicon nanophotonic wire waveguide," arXiv e-print 1405.4205 (2014) .
20. N. Akhmediev and M. Karlsson, "Cherenkov radiation emitted by solitons in optical fibers," Phys. Rev. A **51,** 2602–2607 (1995).
21. M. Erkintalo, Y. Q. Xu, S. G. Murdoch, J. M. Dudley, and G. Genty, "Cascaded phase matching and nonlinear symmetry breaking in fiber frequency combs," Phys. Rev. Lett. **109,** 223904/1–5 (2012).
22. X. Gu, M. Kimmel, A. P. Shreenath, R. Trebino, J. M. Dudley, S. Coen, and R. S. Windeler, "Experimental studies of the coherence of microstructure-fiber supercontinuum," Opt. Express **11,** 2697–2703 (2003).
23. F. Lu and W. Knox, "Generation of a broadband continuum with high spectral coherence in tapered single-mode optical fibers," Opt. Express **12,** 347–353 (2004).
24. D. Türke, S. Pricking, A. Husakou, J. Teipel, J. Herrmann, and H. Giessen, "Coherence of subsequent supercontinuum pulses generated in tapered fibers in the femtosecond regime," Opt. Express **15,** 2732–2741 (2007).
25. J. W. Nicholson, A. D. Yablon, M. F. Yan, P. Wisk, R. Bise, D. J. Trevor, J. Alonzo, T. Stockert, J. Fleming, E. Monberg, F. Dimarcello, and J. Fini, "Coherence of supercontinua generated by ultrashort pulses compressed in optical fibers," Opt. Lett. **33,** 2038–2040 (2008).
26. L. Yin and G. P. Agrawal, "Impact of two-photon absorption on self-phase modulation in silicon waveguides," Opt. Lett. **32,** 2031–2033 (2007).
27. L. Yin, Q. Lin, and G. P. Agrawal, "Soliton fission and supercontinuum generation in silicon waveguides," Opt. Lett. **32,** 391–393 (2007).
28. X. Liu, B. Kuyken, G. Roelkens, R. Baets, R. M. O. Jr, and W. M. J. Green, "Bridging the mid-infrared-to-telecom gap with silicon nanophotonic spectral translation," Nature Photonics **6**, 667 (2012).